Magyarhoni Földtani Társulat
Földtani Közlöny
Hungarian Geological Society

156/3, 277–286., Budapest, 2026

DOI: 10.23928/foldt.kozl.2026.156.3.277

Mineralogical mosaics from the Carpathian–Pannonian region 7

This paper is dedicated to Tamás G. Weiszburg on the occasion of his 70th birthday

Szakáll, Sándor[1,*], Fehér, Béla[2], Kristály, Ferenc[1], Mihály, Judith[3], Bulátkó-Debus, Délia[1], Topa, Boglárka Anna[1], Zajzon, Norbert[1]

[1]Institute of Exploration Geosciences, University of Miskolc, H-3515 Miskolc-Egyetemváros, Hungary
[2]Department of Mineralogy, Herman Ottó Museum, Kossuth u. 13, H-3525 Miskolc, Hungary
[3]HUN-REN Research Centre for Natural Sciences, Institute of Materials and Environmental Chemistry, Magyar tudósok körútja 2, H-1117 Budapest, Hungary

*E-mail: sandor.szakal@uni-miskolc.hu

Ásványtani mozaikok a Kárpát–Pannon régióból 7.

Összefoglalás

Hetedik tanulmányunkban további mozaikszerű információkat közlünk a Kárpát–Pannon régióra vonatkozó új ásványtani kutatási eredményekből. Az adatokat országok és lelőhelyek szerint csoportosítottuk. Az egyes „mozaikdarabokban" az ásványok pontos leírására és – döntően röntgen-pordiffrakció, pásztázó elektronmikroszkóp és elektronmikroszonda általi – meghatározására, valamint a paragenezis tömör bemutatására koncentráltunk. A tanulmányban szereplő ásványok olykor első említések az egész régióból vagy legalábbis az illető lelőhelyről.

Magyarországról a rudabányai érctelepből gerhardtit és parnauit, egy recski mélyfúrásból armenit, a badacsonyörsi uránindikációból zeunerit, valamint a hosszúhetényi fonolit-kőfejtőből polilitionit vizsgálati adatait közöljük.

Romániából a jádremetei metamorf bauxittelepből margarit, a felsőbányai ércesedésből coquandit és mopungit, míg a bánsági Szászkabánya ércesedéséből delafossit jelenlétét dokumentáljuk.

Tárgyszavak: gerhardtit, parnauit, armenit, zeunerit, polilitionit, margarit, coquandit, mopungit, delafossit

Abstract

Further mosaic-like data are presented on the mineral occurrences of the Carpathian–Pannonian region in this seventh paper of the series arranged by countries and localities. Each "mosaic" contains a concise mineral description, mainly based on X-ray powder diffraction, scanning electron microscopy, and electron microprobe analyses, and a brief characterisation of the mineral paragenesis. Some minerals are first-time descriptions from the entire discussed region, but all are newly documented occurrences at least at the described locality.

From Hungary, we present analytical data on gerhardtite and parnauite from the Rudabánya ore deposit, armenite from a borehole at Recsk, zeunerite from the uranium indication in Badacsonyörs, and polylithionite from the phonolite quarry at Hosszúhetény.

From Romania, we document the presence of margarite from the metamorphosed bauxite deposit at Remeți, coquandite and mopungite from the ore deposit at Baia Sprie, and delafossite from the ore deposit at Sasca Montană in the Banat region.

Keywords: gerhardtite, parnauite, armenite, zeunerite, polylithionite, margarite, coquandite, mopungite, delafossite

The minerals described in the paper

Table I lists the minerals described in this paper with their ideal composition, the locality where the mineral was found and also the methods used for their identification. The geographical location of the discussed mineral localities is marked on a schematic geological map of the Carpathian–Pannonian region (*Figure 1*).

Experimental methods and samples

X-ray powder diffraction (XRPD) patterns of armenite, margarite, coquandite, and delafossite were recorded on a Bruker D8 Advance diffractometer using Cu*K*α radiation (40 kV and 40 mA) with a 250 mm-radius goniometer, in parallel-beam geometry obtained by Goebel-mirror optics, 0.25° primary axial Soller with a 0.6 mm divergence slit and

Table I. List of identified minerals with their theoretical formulae, locality, and identification methods. The results of the identification methods in brackets are not published

I. táblázat. *Az azonosított ásványok ideális képletükkel, lelőhelyükkel és az azonosítás módjaival. A zárójelbe tett vizsgálati módszerek mérési eredményeit nem közöljük*

Mineral	Ideal formula	Locality	Identification methods
Armenite	$BaCa_2Al_6Si_9O_{30} \cdot 2H_2O$	Recsk ore deposit, HUN	XRPD, WDX
Coquandite	$Sb^{3+}{}_6O_8(SO_4) \cdot H_2O$	Baia Sprie ore deposit, ROM	XRPD, EDX
Delafossite	$Cu^+Fe^{3+}O_2$	Sasca Montană ore deposit, ROM	XRPD, WDX
Gerhardtite	$Cu_2(NO_3)(OH)_3$	Rudabánya ore deposit, HUN	XRPD, EDX, FTIR
Margarite	$CaAl_2(Al_2Si_2)O_{10}(OH)_2$	Remeți ore deposit, ROM	XRPD, WDX
Mopungite	$NaSb^{5+}(OH)_6$	Baia Sprie ore deposit, ROM	EDX, (XRPD)
Parnauite	$Cu_9(AsO_4)_2(SO_4)(OH)_{10} \cdot 7H_2O$	Rudabánya ore deposit, HUN	XRPD, EDX
Polylithionite	$K(Li_2Al)Si_4O_{10}(F, OH)_2$	Köves Hill, Hosszúhetény, HUN	WDX
Zeunerite	$Cu(UO_2)_2(AsO_4)_2 \cdot 10–16H_2O$	Örsi Hill, Badacsonyörs, HUN	XRPD, (WDX)

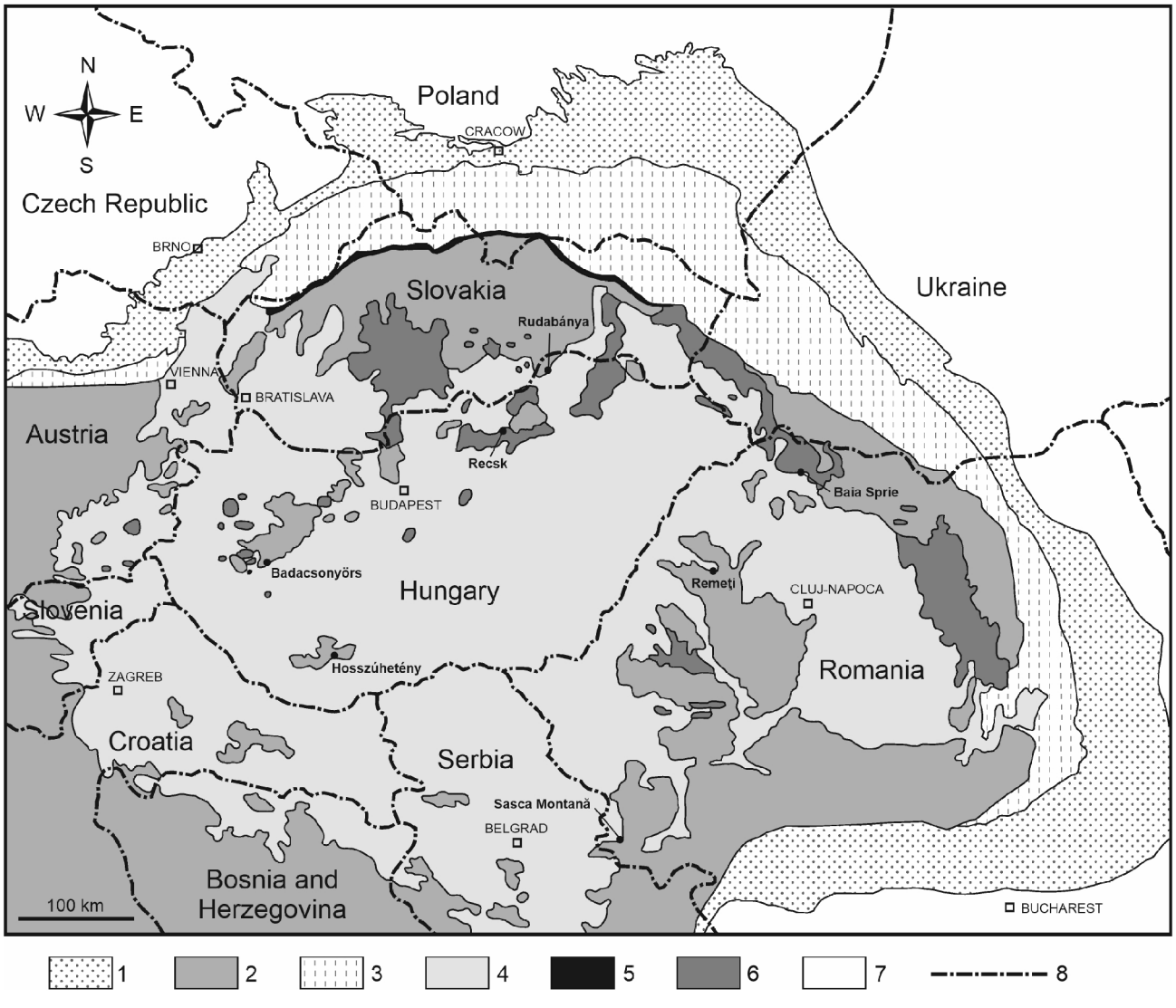


Figure 1. Location of the discussed localities marked on the schematic geological map of the Carpathian–Pannonian region

Legend: 1 = Alpine-Carpathian foredeep; 2 = Inner Alpine, Carpathian and Dinarides units; 3 = Alpine-Carpathian flysch belt; 4 = Neogene basins; 5 = Pieniny Klippen Belt; 6 = neovolcanic areas; 7 = foreland platform areas; 8 = state borders

1. ábra. *A tárgyalt lelőhelyek elhelyezkedése a Kárpát-Pannon régió vázlatos földtani térképén*

Jelmagyarázat: 1 = Alpi-Kárpáti előmélyedés; 2 = Belső-Alpi, Kárpáti és Dinári egységek; 3 = Alpi-Kárpáti flisöv; 4 = neogén medencék; 5 = Pieniní-szirtöv; 6 = neovulkáni területek; 7 = előtéri platformterületek; 8 = országhatárok

position sensitive Vantec-1 detector (1° opening). Samples of 1 to 5 mg were ground in agate mortar under acetone and loaded on low-background (Si crystal) sample holders. All patterns were recorded in the 2–70° (2θ) range at a scanning rate of 0.007° (2θ) per 4 s.

X-ray diffraction study was also performed with a 114.6 mm diameter Gandolfi camera for gerhardtite, parnauite, and zeunerite. Analytical parameters: Cu*K*α radiation, Ni filter, 40 kV accelerating voltage, 20–35 mA tube current, and 44–70 h exposure time. Unit cell parameters were calculated with the UnitCell software (Holland & Redfern 1997).

Scanning electron microscopy (SEM) studies and energy-dispersive X-ray spectroscopy (EDX) were performed using a JEOL JXA-8600 Superprobe instrument equipped with an EDX silicon drift detector (SDD) at the Institute of Exploration Geosciences, University of Miskolc. For the EDX measurements 15–20 kV accelerating voltage was used, with a probe current of 10–20 nA. A 4 × 5 μm area was scanned with a focused beam during the analyses (stopped focused beam was used if the target area was too small).

Quantitative electron-microprobe analyses (EMPA) were performed at the Geological Institute of Dionýz Štúr, Bratislava, Slovakia. For analyses of armenite, zeunerite, polylithionite, margarite, and delafossite, a Cameca SX-100 instrument was used in wavelength-dispersive mode (WDX). Operating conditions were as follows: accelerating voltage 15 kV, probe current 20 nA. Analytical standards: pyrite (S), apatite (P), GaAs (As), SiO_2 (Si), TiO_2 (Ti), UO_2 (U), Al_2O_3 (Al), Cr_2O_3 (Cr), fayalite (Fe), MgO or forsterite (Mg), wollastonite (Ca), rhodonite (Mn), Ni metal (Ni), Cu metal (Cu), Zn metal (Zn), $SrTiO_3$ (Sr), baryte (Ba), albite (Na), orthoclase (K), CaF_2 (F), and NaCl (Cl). Raw intensity data were corrected using a PAP matrix correction.

The infrared (IR) spectrum of gerhardtite was recorded using the Attenuated Total Reflection (ATR) technique by means of a Varian Scimitar 2000 Fourier-transform infrared (FTIR) spectrometer (Varian Inc., US) fitted with a Mercury-Cadmium-Telluride (MCT) detector. The ATR accessory was a "Golden Gate" (SPECAC Ltd., UK) single-reflection diamond ATR with an active area of 0.6 × 0.6 mm^2. For the measurement, usually a 50 μg sample (a few grains) was used without any further sample preparation. The grains were carefully transported onto the surface of the diamond ATR element and pressed by a sapphire anvil to ensure good contact between the ATR optical element and the sample to acquire spectra with sufficient signal-to-noise ratio. Due to the ATR diamond absorbance around 1900–2600 cm^{-1}, this wavenumber region was excluded from the evaluation, however, only thiol, nitrile, thiazide, and azide groups have bands in this region. In all cases, the reflection spectra are ATR corrected (Varian ResolutionPro 4.0 software), allowing comparison with reference transmission spectra.

The presence of lithium in the polylithionite sample was confirmed using a handheld Laser Induced Breakdown Spectrometer (LIBS) at the Institute of Exploration Geosciences, University of Miskolc. A SciAps Z-903 instrument was used with the following operating conditions: 1064 nm excitation laser, pulse energy: 5–6 mJ/pulse, argon flush.

All investigated samples are deposited in the mineral collection of the Herman Ottó Museum, Miskolc, Hungary (inventory numbers: 2012.190 for gerhardtite and parnauite, Rudabánya; 2021.30 for armenite, Recsk; 2011.171 for zeunerite, Badacsonyörs; 2023.116 for polylithionite, Hosszúhetény; 2025.58 for margarite, Remeți; 2023.117 for coquandite and mopungite, Baia Sprie; and 2026.1 for delafossite, Sasca Montană).

Results

Hungary

Gerhardtite and parnauite from Rudabánya ore deposit

A massive cuprite specimen was recovered from an unknown part of the oxidation zone of the Rudabánya ore deposit, in which a rare copper nitrate hydroxide (gerhardtite) and a hydrous copper arsenate sulphate hydroxide (parnauite) were detected, along with malachite and azurite vein fillings. The most common mineral is malachite, which forms spherical encrustations on the walls of the 0.5–1 cm-sized cavities. The light green, columnar or lath-shaped crystals of parnauite up to 0.1 mm in length were observed much rarely (*Figure 2*). Among the cavity filling phases, gerhardtite is the youngest mineral, which appears as emerald green or bluish green, tabular crystals reaching 1–3 mm in diameter (*Figure 3*). The excellent cleavage of gerhardtite on {001} is clearly visible, the cleavage surface has a slightly pearly lustre. Both minerals were determined based on XRPD patterns (*Tables E1–E2* – see the electronic supplementary material). The lattice constants calculated from the XRPD data were $a = 5.80(1)$, $b = 6.11(1)$, $c = 13.81(2)$ Å and $V = 471(1)$ $Å^3$ for gerhardtite and $a = 14.93(3)$, $b = 14.126(8)$, $c = 6.03(3)$ Å and $V = 1272(5)$ $Å^3$ for parnauite. The qualitative elemental com-

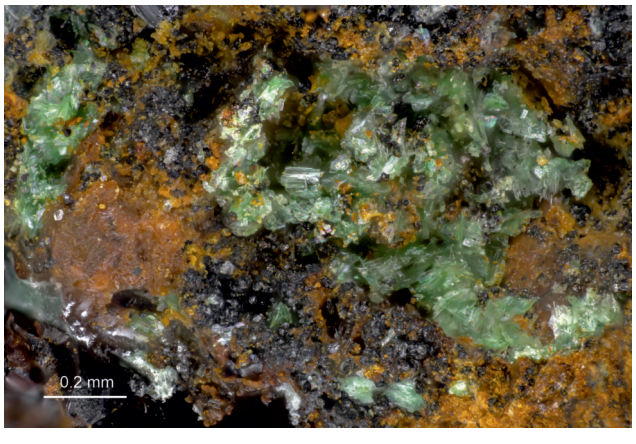


Figure 2. Light green parnauite crystals, Rudabánya. Field of view: 1.5 mm. Collection of the Herman Ottó Museum (HOM). Photo courtesy of G. Koller

2. ábra. *Parnauit világoszöld kristályai, Rudabánya. Képszélesség: 1,5 mm. Herman Ottó Múzeum (HOM) gyűjteménye. Fotó: Koller G.*

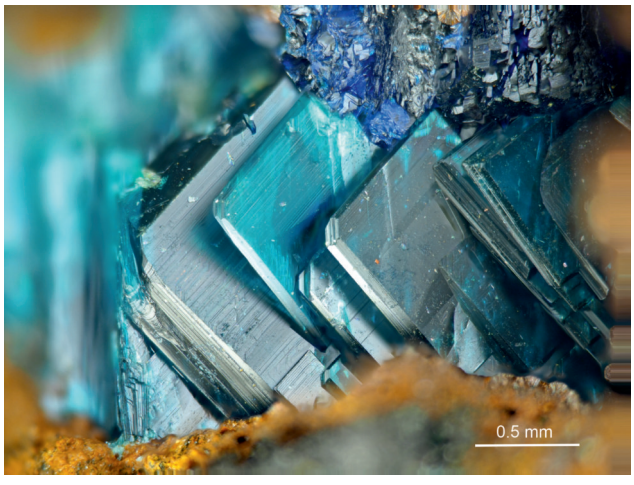


Figure 3. Bluish green, tabular gerhardtite crystals, Rudabánya. Field of view: 3 mm. G. KOLLER's collection. Photo courtesy of L. TÓTH

3. ábra. *Kékeszöld, táblás gerhardtitkristályok, Rudabánya. Képszélesség: 3 mm. KOLLER G. gyűjteménye. Fotó: TÓTH L.*

position of the minerals was determined by EDX. FTIR spectroscopy was also used to identify gerhardtite (*Figure 4*). Its IR bands agreed well with the data compiled by FU et al. (2020) for the synthetic counterpart. The observed absorption bands were at 464 (ν Cu–O), 510 (ν Cu–O), 667 (δ_1 CuOH), 783 (δ_2 CuOH), 867 (δ_3 CuOH), 1045 (ν_1 NO_3), 1320 (ν_3 NO_3), 1413 (ν_3 NO_3), 1766 ($\nu_1 + \nu_4$ NO_3), 2748, 2850 (sum or difference frequencies of some normal modes), 3401 (ν_{s3} OH) and 3523 cm^{-1} (ν_{s1} OH). The formation of gerhardtite in the oxidation zone of the ore deposit, similarly to the more common chlorides, bromides and iodides, presumably occurred in an arid climate. The elevated nitrogen is likely the result of hydrothermal mobilization of nitrogen from organic matter associated with sedimentary host-rock.

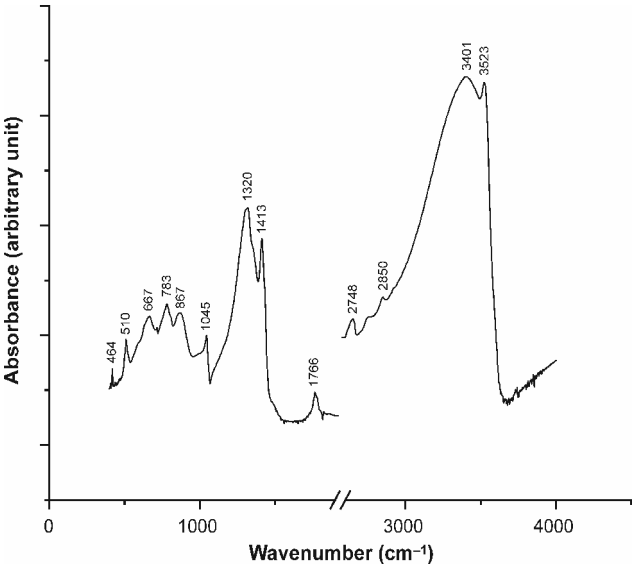


Figure 4. FTIR spectrum of gerhardtite, Rudabánya. The range between 1900–2600 cm^{-1} is cut out due to the strong phonon band absorption of diamond

4. ábra. *A rudabányai gerhardtit FTIR-spektruma. Az 1900–2600 cm^{-1} közötti tartomány kivágva a gyémánt erős fononsáv-abszorpciója miatt*

Armenite from Recsk ore deposit

After chayesite, osumilite, osumilite-(Mg) and roedderite, armenite is the fifth member from the milarite group to be detected in the territory of Hungary. This phase was found in a striking, pink-mottled, strongly silicified rock extracted from the 193rd meter of the borehole Rm-73 in Recsk. The groundmass of this pyrite- and chalcopyrite-bearing rock is predominantly composed of quartz and calcite, and the rock is related to the deep-level ore formation. The pink nests and vein fillings received their colour from Mn-containing clinozoisite ("clinothulite" variety). This phase can be observed as scattered or intimately intergrown prismatic crystals and can form nodules up to 1 cm in size. Armenite itself can be recognized as hexagonal crystals up to 150 μm in size (*Figure 5*). Based on microprobe analyses, its chemical composition is close to the ideal ($BaCa_2Al_6Si_9O_{30} \bullet 2H_2O$), and it does not show chemical inhomogeneity (*Table II*). During the measurement, some water was escaped from the mineral, so if the water content is calculated from the difference between the analytical totals and 100%, then only 1.10–1.57 water molecules are found per formula unit instead of the ideal 2. The identification of armenite is also supported by the XRPD pattern (*Table E3* – see the electronic supplementary material). The armenite crystals are strongly fractured and contain many clinozoisite inclusions. In its wider environment, andradite/grossular, apatite, anhydrite, baryte, and sulphides (pyrite, chalcopyrite, galena, sphalerite) can be observed in the exoskarn.

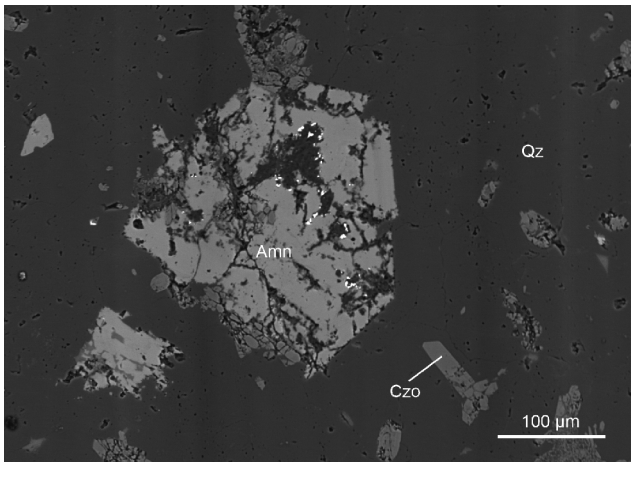


Figure 5. Hexagonal armenite (Amn) and columnar clinozoisite (Czo) in quartz (Qz). Recsk. BSE image

5. ábra. *Hatszöges armenit (Amn) és oszlopos klinozoisit (Czo) kvarcban (Qz). Recsk. Visszaszórtelektron-kép*

Zeunerite from Badacsonyörs uranium occurrence

Uranium mineral occurrences were discovered in the late 1950s in the Permian pyrite-bearing grey sandstone on Örsi Hill near Badacsonyörs (MAJOROS 1960). To investigate this mineralization, an exploration adit was driven to intersect the pyrite-bearing zones, which were richest also in uranium oxides. Pyrite is closely intergrown with fine-grained uranium

Table II. Electron-microprobe analyses of armenite from Recsk in wt%
II. táblázat. *A recski armenit elektronmikroszondás elemzései tömegszázalékban*

	(1)	(2)	(3)	(4)	(5)
SiO_2	47.70	48.34	47.99	48.00	48.23
Al_2O_3	27.04	26.44	26.54	26.91	26.68
MgO	0.00	0.00	0.00	0.00	0.00
CaO	10.16	9.61	9.93	10.09	10.03
MnO	0.02	0.01	0.01	0.00	0.00
FeO	0.00	0.01	0.01	0.00	0.03
SrO	0.15	0.04	0.05	0.12	0.26
BaO	12.72	12.92	12.43	12.79	12.12
Na_2O	0.07	0.38	0.15	0.10	0.09
K_2O	0.27	0.27	0.41	0.25	0.37
H_2O*	1.87	1.97	2.49	1.76	2.19
Total	**100.00**	**100.00**	**100.00**	**100.00**	**100.00**
Cation numbers based on 30 oxygens / Kationszámok 30 oxigénre számolva					
Si	8.98	9.10	9.06	9.02	9.06
Al	6.00	5.87	5.91	5.96	5.91
Mg	0.00	0.00	0.00	0.00	0.00
Ca	2.05	1.94	2.01	2.03	2.02
Mn	0.00	0.00	0.00	0.00	0.00
Fe	0.00	0.00	0.00	0.00	0.00
Sr	0.02	0.00	0.01	0.01	0.03
Ba	0.94	0.95	0.92	0.94	0.89
Na	0.03	0.14	0.05	0.04	0.03
K	0.06	0.06	0.10	0.06	0.09
H_2O	1.17	1.24	1.57	1.10	1.37

*H_2O calculated from the difference between the analytical total and 100% / *H_2O az analitikai összegek és a 100% különbségéből számolva*

oxides (soot-like type) and is generally found at their margins. Most often pyrite also contains a few percent Se and/or As. Sphalerite and chalcopyrite are less common among the sulphides of the sandstone. Next to them, sulphates and arsenates were formed near the surface due to oxidation processes. Gypsum and jarosite are the predominant minerals, while scorodite (spherical aggregates composed of brown, stout prisms) and zeunerite are less common. Majoros (1960) and Kiss (1961) mentioned several other phosphates and arsenates, of which saléeite is considered valid based on XRPD and chemical analysis. Among the secondary minerals, a tiny phase, characterized by purple coatings, is rarely found, which is similar to downeyite based on elemental composition (Se and O content) and Raman spectra (due to the minute size of the sample, further studies could not be performed). Green zeunerite is a weathering product appearing at the margins of pyrite and uranium oxide nodules. Its tabular crystals reach 0.1 mm (*Figure 6*), they are often grouped into fan-shaped aggregates. The XRPD pattern (*Table E4* – see the electronic supplementary material) support its identification. The lattice constants calculated from the XRPD data are $a = 7.190(6)$, $c = 20.80(2)$ Å and $V = 1076(2)$ Å^3. Several attempts were made to quantitatively determine the chemical composition of zeunerite using electron microprobe, but during the measurements some of the weakly bound copper ions always left, even when the sample current was reduced to 10 nA. For this reason, the Cu:As ratio in the empirical



Figure 6. Green, tabular crystal of zeunerite, Badacsonyörs. Field of view: 1 mm. S. Klaj's collection. Photo courtesy of L. Tóth

6. ábra. *Zeunerit zöld, táblás kristálya, Badacsonyörs. Képszélesség: 1 mm. Klaj S. gyűjteménye. Fotó: Tóth L.*

formula was always much lower than the theoretical value (1:2). The strong destruction of the crystals after the microprobe analyses was also clearly observed in the BSE images.

Polylithionite from Hosszúhetény phonolite quarry

Polylithionite forms colourless or pale blue, usually 0.2–0.4 mm plates (rarely reaching 2 mm) and tangled scaly aggregates in the miarolitic cavities of the phonolite of the Köves-tető quarry at Hosszúhetény (*Figure 7*). Its fan- or rosette-shaped crystal groups are also characteristic. Among the miarolitic phases, the larger (up to 1–3 mm) hydrothermal REE minerals are also noteworthy. They are the products of the remobilization of the primary, submicroscopic (a few micrometers in size) REE phases of phonolite (Szakáll et al. 2014). Fluorine- and chlorine-containing fluids, which play an important role in the formation of miarolitic cavities, also resulted in the formation of lithium mica and fluorite ap-

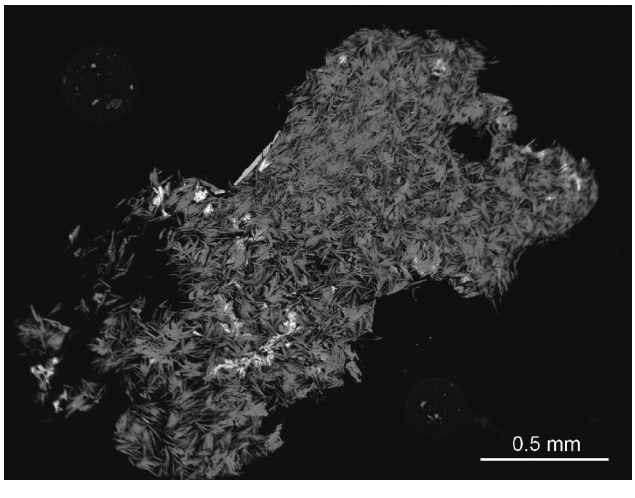


Figure 7. Scaly aggregate of polylithionite, Hosszúhetény. BSE image. Photo courtesy of V. Kollárová

7. ábra. *Polilitionit pikkelyes halmaza, Hosszúhetény. Visszaszórtelektron-kép. Fotó: V. Kollárová*

pearing in the closer environments. The scaly aggregates of polylithionite are found in miarolitic cavities, often completely filled with natrolite, together with aegirine and albite. It is clearly observed that the lithium mica formed earlier than natrolite, as their plates are covered with the zeolite. In its immediate vicinity, among the REE phases, minute, yellowish aggregates of calcioancylite-(Ce) and ancylite-(Ce) appear. A thin smectite or manganese oxide coating can occasionally be observed on the surface of the crystals. The Hosszúhetény polylithionite was previously considered to be muscovite, but the fluorine peak appearing in the EDX spectrum, the high Si:Al ratio compared to that of muscovite, and the minimal Fe and Mg content clearly indicated that we are dealing with a Li-containing mica, a member of the lepidolite series. Although lithium cannot be measured with an electron microprobe, its amount can be easily calculated from crystal-chemical considerations (*Table III*). Based on the calculations, the Li:Al ratio in the octahedral sheet is 2:1, and Si = 4 apfu in the tetrahedral sheet, which corresponds to the composition of polylithionite. This is markedly different from the composition of the other member of the lepidolite series, trilithionite, where the Li:Al ratio is 1:1 and the tetrahedral sheet contains 3 apfu Si + 1 apfu Al. Otherwise, the presence of lithium in the phase was confirmed by a handheld laser-induced breakdown spectrometer (LIBS). Lithium was detected in every measurement, commonly as a major constituent.

Table III. Electron-microprobe analyses of polylithionite from Hosszúhetény in wt.%

III. táblázat. *A hosszúhetényi polilitionit elektronmikroszondás elemzései tömegszázalékban*

	(1)	(2)	(3)	(4)
SiO_2	59.66	60.95	61.66	61.20
TiO_2	0.31	0.36	0.50	0.37
Al_2O_3	13.83	12.65	12.50	13.37
FeO*	1.28	0.86	1.33	1.31
MnO	0.13	0.07	0.25	0.11
MgO	0.04	0.00	0.00	0.09
CaO	0.00	0.00	0.00	0.07
Li_2O**	7.20	7.50	7.50	7.35
Na_2O	0.10	0.11	0.21	0.13
K_2O	11.02	11.58	11.52	11.22
H_2O***	0.80	0.28	0.60	0.70
F	7.93	9.07	8.50	8.28
O=F	-3.34	-3.82	-3.58	-3.49
Total	**98.96**	**99.61**	**100.99**	**100.71**
Ion numbers based on 12 anions (O, OH, F) Ionszámok 12 anionra (O, OH, F) számolva				
Si	3.93	3.99	3.99	3.96
Al^{iv}	0.07	0.01	0.01	0.04
Σ*T*	**4.00**	**4.00**	**4.00**	**4.00**
Al^{vi}	1.00	0.96	0.94	0.98
Ti	0.02	0.02	0.02	0.02
Fe^{2+}	0.07	0.05	0.07	0.07
Mn	0.01	0.00	0.01	0.01
Mg	0.00	0.00	0.00	0.01
Li	1.90	1.97	1.95	1.92
Σ*M*	**3.00**	**3.00**	**3.00**	**3.00**
Ca	0.00	0.00	0.00	0.00
Na	0.01	0.01	0.03	0.02
K	0.93	0.97	0.95	0.93
Σ*I*	**0.94**	**0.98**	**0.98**	**0.95**
OH	0.35	0.12	0.26	0.30
F	1.65	1.88	1.74	1.70
Σ*X*	**2.00**	**2.00**	**2.00**	**2.00**

* Total iron measured as FeO. / *Összes vas FeO-ként mérve.*

** Li_2O calculated from the stoichiometry: M = 3 apfu. / *Li_2O a sztöchiometrikus összetételből számolva: M = 3 apfu.*

*** H_2O calculated from the stoichiometry: F + OH = 2 apfu. / *H_2O a sztöchiometrikus összetételből számolva: F + OH = 2 apfu.*

While trilithionite is predominantly associated with granite pegmatites, polylithionite is not rare in alkaline igneous rocks either. Numerous occurrences are known in nepheline syenite pegmatites and in the miarolitic cavities of phonolites (its type locality in Greenland occurs in nepheline syenite; LORENZEN 1884). In the nepheline syenite pegmatite of Mont Saint-Hilaire, Canada, it is accompanied by aegirine, albite, analcime, and natrolite (HORVÁTH et al. 2019). In the miarolitic cavities of the Aris phonolite quarry in Namibia, albite, aegirine, and natrolite are also the most common associates (KOLITSCH et al. 2016).

Romania

Margarite in metamorphosed bauxite from Remeți (Jádremete) ore deposit

SZÁDECZKY (1905) was certainly the first to mention margarite under the name "white mica" from the margin of the Izvor bauxite deposit in Remeți. He described this rare rock-forming mineral in dark-coloured bauxites, which were considered to have suffered contact metamorphism. He observed chlorite and quartz in its vicinity in thin sections. It is also worth mentioning that Pál ROZLOZSNIK collected well-developed diaspore crystals in the bauxite mine operating in the Valea Izvor area around 1915. In his paper focusing on field observations, ROZLOZSNIK (1917) only wrote: "the extremely hard rock acquires a dark black colour, where beautiful coatings of diaspore crystals have formed in its cracks". One of the outstandingly developed types of diaspore occurs as nests of 1–3 cm-sized, white, pearly scales, while another type can be observed in the form of brown, columnar crystals reaching 4 cm. Around 2005, in Valea Izvor, near the mouth of the Iadu stream, in an old ore dump, several contact metamorphosed bauxite specimens were found in which the "white mica" showed a varied appearance (fine-scaled, coarse-scaled, and lath-like aggregates). It is worth mentioning that this ore dump could no longer be found in 2025. All these types of "white mica" were clearly proved to be margarite based on the XRPD data (*Table E5* – see the electronic supplementary material) and chemical analyses (*Table IV*). The lattice constants calculated from the XRPD data are a = 5.11(1), b = 8.78(3), c = 19.35(2) Å, β = 95.6(2)° and V = 865(2) Å^3. According to the textural images, margarite often grows together with chamosite and its occurrence is particu-

Table IV. Electron-microprobe analyses of margarite from Remeți in wt%
IV. táblázat. *A jádremetei margarit elektronmikroszondás elemzései tömegszázalékban*

	(1)	(2)	(3)	(4)	(5)	(6)
SiO_2	30.30	30.76	35.72	35.81	33.77	30.47
Al_2O_3	50.83	50.86	47.30	47.24	48.98	50.73
MgO	0.00	0.00	0.00	0.04	0.00	0.00
CaO	13.62	13.30	10.87	10.42	12.08	13.58
FeO*	0.41	0.54	0.51	0.47	0.49	0.52
Na_2O	0.16	0.43	0.46	0.44	0.34	0.30
K_2O	0.02	0.06	0.63	0.56	0.34	0.03
H_2O**	4.52	4.53	4.57	4.57	4.57	4.52
Total	**99.86**	**100.49**	**100.06**	**99.56**	**100.58**	**100.15**
Cation numbers based on 12 oxygens / Kationszámok 12 oxigénre						
Si	2.01	2.03	2.34	2.35	2.21	2.02
Al	1.99	1.97	1.66	1.65	1.79	1.98
Σ*T*	**4.00**	**4.00**	**4.00**	**4.00**	**4.00**	**4.00**
Al	1.99	1.99	1.99	2.01	1.99	1.98
Fe	0.02	0.03	0.03	0.03	0.03	0.03
Mg	0.00	0.00	0.00	0.00	0.00	0.00
Σ*M*	**2.01**	**2.02**	**2.02**	**2.04**	**2.02**	**2.01**
Ca	0.97	0.94	0.76	0.73	0.85	0.96
Na	0.02	0.06	0.06	0.06	0.04	0.04
K	0.00	0.01	0.05	0.05	0.03	0.00
Σ*I*	**0.99**	**1.01**	**0.87**	**0.84**	**0.92**	**1.00**

Other measured, but undetected elements: F, Cl, Mn, Ni, Cr, Ti / *Egyéb mért, de nem detektált elemek: F, Cl, Mn, Ni, Cr, Ti*
* Total iron was measured as FeO. / *Összes vas FeO-ként mérve*
** H_2O calculated from the stoichiometry: OH = 2 apfu / *H_2O a sztöchiometrikus összetételből számolva: OH = 2 apfu*

larly characteristic of the fine-grained, hematite-bearing groundmass (*Figure 8*). In our experience, margarite appears most frequently in dark reddish-brown, hard, compact bauxite. In contrast, the characteristic color of the dark green bauxite examined from the same site is due to chamosite, while that of the black bauxite is due to magnetite; margarite could not be identified in these latter two types.

Coquandite and mopungite from Baia Sprie (Felsőbánya) ore deposit

In the near-surface zones of the Baia Sprie ore deposit, yellow, yellowish-white, or white weathering products of stibnite have been well known for several centuries. Previous data discussed these antimony oxides under the names cervantite and stibiconite (Rădulescu & Dimitrescu 1966). It is worth mentioning that a new antimony sulphate mineral species, klebelsbergite, was described from this ore mineralization (Zsivny 1929). In the past two decades, in addition to klebelsbergite, the following secondary, Sb-containing phases have been confirmed by instrumental studies: cervantite, coquandite, mopungite, stibiconite, sénarmontite, and valentinite. In our experience, these phases always occur in close association with stibnite, mostly in the form of thin crusts, acicular-radial or scaly aggregates (cervantite, coquandite, klebelsbergite, stibiconite), or mostly in the form of euhedral single crystals (sénarmontite, valentinite, mopungite).

Below, we briefly present the previously unpublished coquandite and mopungite. Coquandite forms pale yellow, pearly coatings consisting of 10–20 μm-sized scales on the surface of stibnite crystals (*Figure 9*). These coatings can cover crystal groups larger than 20 cm, making them the largest known occurrence of coquandite in the world. Its determination is confirmed by XRPD data (*Table E6* – see the electronic supplementary material) and EDX analysis (detection of Sb, S and O). The lattice constants calculated from the XRPD data are $a = 11.43(2)$, $b = 29.92(3)$, $c = 11.29(2)$ Å,

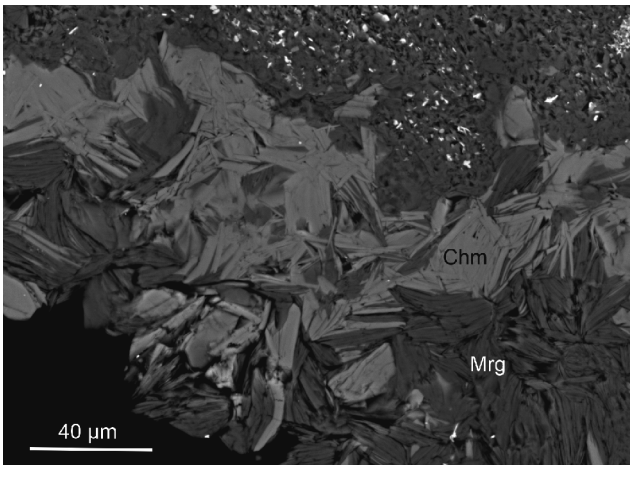


Figure 8. Tabular crystals of margarite (Mrg) and chamosite (Chm), Remeți. BSE image
8. ábra. *Margarit (Mrg) és chamosit (Chm) táblás kristályai, Jádremete. Visszaszórtelektron-kép*

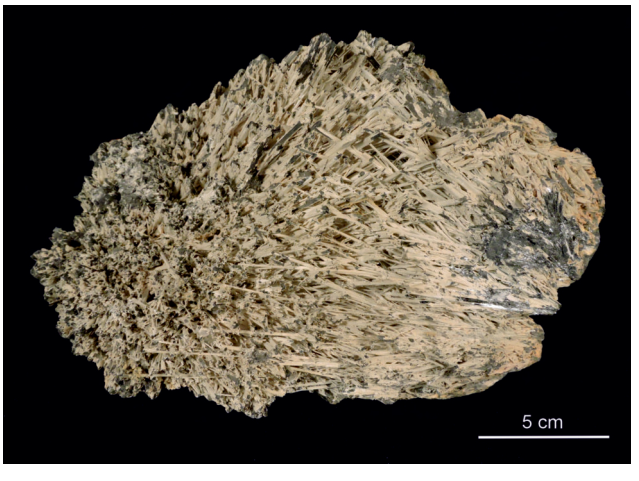


Figure 9. Acicular stibnite crystals covered by pale yellow coquandite, Baia Sprie. Length of the specimen: 22 cm. HOM collection
9. ábra. *Tűs antimonitkristályokat bevonó, halványsárga coquandit, Felsőbánya. A példány 22 cm hosszú. HOM gyűjteménye*

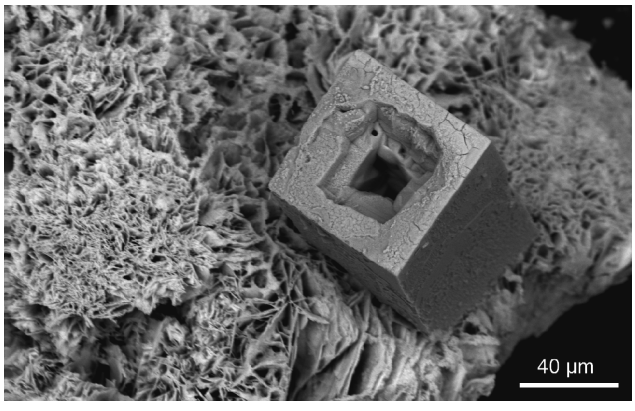


Figure 10. Stubby columnar mopungite crystal on scaly coquandite, Baia Sprie. BSE image. Photo courtesy of Á. KOVÁCS

10. ábra. *Zömök, oszlopos mopungitkristály pikkelyes coquanditon, Felsőbánya. Visszaszórtelektron-kép. Fotó: KOVÁCS Á.*

$\alpha = 91.2(2)°$, $\beta = 119.1(1)°$, $\gamma = 93.1(1)°$ and $V = 3364(6)$ Å^3. Mopungite is rarely observed as colourless, tetragonal prismatic crystals with adamantine lustre – reaching up to 0.5 mm in size – on the surface of weathered stibnite. Its presence is confirmed by EDX analysis (detection of Na, Sb and O). Its stubby columnar crystals sometimes show a skeletal form (*Figure 10*).

Delafossite from Sasca Montană (Szászkabánya) ore deposit

The Sasca Montană copper ore deposit in the Banat region is noteworthy from both mining historical and mineralogical point of view. The extensive presence of an oxidation zone with a high metal content has supported mining operations for several millennia. A new addition to the mineral richness is the detection of the trigonal copper-iron oxide, delafossite. Its presence is related to the limonitic ore type, in which it forms black compact masses. On the walls of smaller cavities, 20–40 µm-sized, slightly distorted scalenohedra can be observed in densely arranged groups (*Figure 11*). The BSE images indicate rhythmic precipitations and

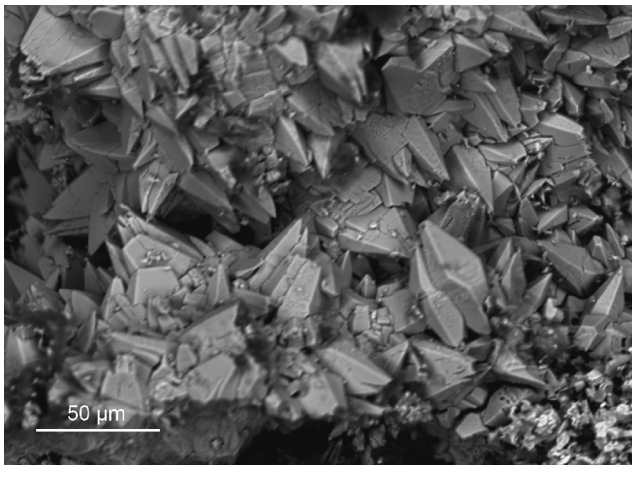


Figure 11. Scalenohedral crystals of delafossite, Sasca Montană. BSE image

11. ábra. *Delafossit szkalenoéderes kristályai, Szászkabánya. Visszaszórtelektron-kép*

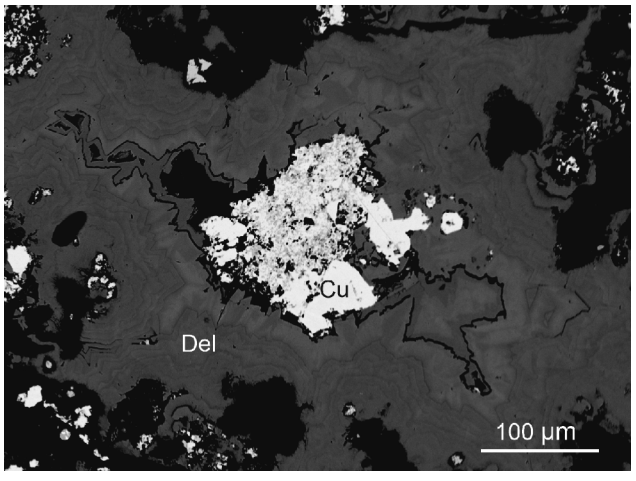


Figure 12. Native copper aggregate (Cu) in chemically zoned delafossite (Del), Sasca Montană. BSE image. Photo courtesy of V. KOLLÁROVÁ

12. ábra. *Természéz-aggregátum (Cu) kémiailag zónás delafossitban (Del), Szászkabánya. Visszaszórtelektron-kép. Fotó: V. KOLLÁROVÁ*

slight chemical zoning, which may have resulted from changes in the Cu:Fe ratio during the formation of the mineral. Native copper often appears within delafossite as irregular aggregates (*Figure 12*). The chemical analyses of delafossite gave values approaching the theoretical composition (*Table V*). The identification was also supported by XRPD pattern (*Table E7* – see the electronic supplementary material). In the close association, cuprite and malachite can also be observed. The mineral assemblage originates from the oxidation of copper sulphides and reflects periodic fluctuations in oxidative-reductive conditions.

Table V. Electron-microprobe analyses of delafossite from Sasca Montană in wt%

V. táblázat. *A szászkabányai delafossit elektronmikroszondás elemzései tömegszázalékban*

	(1)	(2)	(3)	(4)	(5)
SiO_2	0.02	0.01	0.05	0.03	0.07
Al_2O_3	0.34	2.33	1.78	0.31	2.14
Fe_2O_3*	52.09	49.13	50.38	52.43	50.37
MgO	0.00	0.00	0.02	0.00	0.01
Cu_2O**	45.81	45.67	45.74	45.42	45.95
Total	**98.26**	**97.13**	**97.97**	**98.20**	**98.53**
Cation numbers based on 2 oxygens / Kationszámok 2 oxigénre					
Si	0.00	0.00	0.00	0.00	0.00
Al	0.01	0.07	0.05	0.01	0.06
Fe	1.00	0.94	0.96	1.00	0.95
Mg	0.00	0.00	0.00	0.00	0.00
Cu	0.98	0.97	0.97	0.97	0.96

* Total iron was measured as Fe_2O_3 / *Összes vas Fe_2O_3-ként mérve*
** Total copper was measured as Cu_2O / *Összes réz Cu_2O-ként mérve*

Acknowledgements

We thank Bálint Péterdi (Supervisory Authority of Regulatory Affairs, Budapest) for his help by selecting suitable diaspore samples for the investigations. Many thanks to Gábor Koller (Pilisborosjenő), who provided us with gerhardtite, coquandite, and delafossite specimens. The polylithionite samples were submitted for testing by Csaba Papp (Pécs). We also thank the two reviewers, Gábor Papp (Hungarian Natural History Museum, Budapest), and an anonymous reviewer for improvements and comments on the manuscript.

References – Irodalom

Fu, J., Liu, X., Liu, L., Meng, H. & Wang, X. 2020: Infrared and Raman spectral analysis of the polycrystalline copper hydroxonitrates. – *IOP Conference Series: Materials Science and Engineering* **774**, 012060. https://doi.org/10.1088/1757-899X/774/1/012060

Holland, T. J. B. & Redfern, S. A. T. 1997: Unit cell refinement from powder diffraction data: The use of regression diagnostics. – *Mineralogical Magazine* **61**, 65–77. https://doi.org/10.1180/minmag.1997.061.404.07

Horváth, L., Gault, R. A., Pfenninger-Horváth, E. & Poirier, G. 2019: *Mont Saint-Hilaire: History, geology, mineralogy.* – The Canadian Mineralogist Special Publication 14. Mineralogical Association of Canada, 644 p.

Kiss, J. 1961: *The mineralogical composition and genesis of the Mecsek uranium ore deposit [A mecseki uránérctelep ásványos alkata és genezise].* – CSc Theses, Repository of the Hungarian Academy of Sciences, Budapest (in Hungarian).

Kolitsch, U., Blass, G., Jahn, S., Cámara, F., von Bezing, L., Wartha, R. R., Tremmel, G., Sturla, M., Cerea, P., Skebo, M. & Ciriotti, M. E. 2016: *Aris. Mineralogy of the famous alkaline phonolite.* – Associazione Micromineralogica Italiana, Cremona, 95 p.

Lorenzen, J. 1884: Untersuchung einiger Mineralien aus Kangerdluarsuk in Grönland. – *Zeitschrift für Krystallographie* **9**, 243–254. https://doi.org/10.1524/zkri.1884.9.1.243

Majoros, Gy. 1960: *Mineralogical and petrological characteristics of the Permian uranium occurrence in Badacsonyörs [A badacsonyörsi perm uránelőfordulás ásvány-kőzettani jellemzése].* – Manuscript, Repository of Mecsekérc Zrt., Pécs (in Hungarian).

Rădulescu, D. & Dimitrescu, R. 1966: *Topographical mineralogy of Romania [Mineralogia topografică a României].* – Editura Academiei Republicii Socialiste România, Bucureşti, 376 p. (in Romanian).

Rozlozsnik, P. 1917: Preliminary report on the conditions of occurrence of bauxite in northern Bihar (Királyerdő) [Előzetes jelentés a bauxit előfordulási körülményeiről az északi Biharban (Királyerdőben)]. – *A Magyar Királyi Földtani Intézet Évi Jelentése az 1916. évről*, 450–454 (in Hungarian).

Szádeczky, Gy. 1905: About the aluminum ores of the Bihar Mountains [A Biharhegység alumíniumérceiről]. – *Földtani Közlöny* **35**, 213–231 (in Hungarian).

Szakáll, S., Jáger, V., Fehér, B. & Zajzon, N. 2014: Rare earth elements and their minerals in the Mecsek phonolite [A mecseki fonolit ritkaföldfémtartalma és ásványi hordozói]. – In: Szakáll, S. (Ed.): *Rare earth elements in Hungarian geological formations [Ritkaföldfémek magyarországi földtani képződményekben].* CriticEl Monography Series No. 5, Milagrossa Kft., Miskolc, 47–66 (in Hungarian).

Zsivny, V. 1929: Klebelsbergite, a new mineral from Felsőbánya [Klebelsbergit, egy új ásvány Felsőbányáról]. – *Mathematikai és Természettudományi Értesítő* **46**, 19–26 (in Hungarian).

Manuscript received: 2026/06/25

Electronic supplementary materials

Table E1. X-ray powder diffraction data of gerhardtite from Rudabánya compared to the reflections of the ICDD 00-014-0687 card
E1. táblázat. *A rudabányai gerhardtit röntgen-pordiffrakciós adatai, összehasonlítva az ICDD 00-014-0687 kártya reflexióival*

Table E2. X-ray powder diffraction data of parnauite from Rudabánya in comparison with those of the ICDD 00-029-0533 card
E2. táblázat. *A rudabányai parnauit röntgen-pordiffrakciós adatai, összehasonlítva az ICDD 00-029-0533 kártya megfelelő reflexióival*

Table E3. X-ray powder diffraction data of an armenite-bearing sample from Recsk
E3. táblázat. *A recski armenittartalmú minta röntgen-pordiffrakciós adatai*

Table E4. X-ray powder diffraction data of zeunerite from Badacsonyörs in comparison with the corresponding reflections of the ICDD 00-017-0150 card
E4. táblázat. *A badacsonyörsi zeunerit röntgen-pordiffrakciós adatai, összehasonlítva az ICDD 00-017-0150 kártya megfelelő reflexióival*

Table E5. X-ray powder diffraction data of margarite from Remeți compared to the reflections of the ICDD 00-018-0276 card

E5. táblázat. *A jádremetei margarit röntgen-pordiffrakciós adatai, összehasonlítva az ICDD 00-018-0276 kártya reflexióival*

Table E6. X-ray powder diffraction data of coquandite from Baia Sprie compared to the reflections of the ICDD 00-046-1417 card
E6. táblázat. *A felsőbányai coquandit röntgen-pordiffrakciós adatai, összehasonlítva az ICDD 00-046-1417 kártya reflexióival*

Table E7. X-ray powder diffraction data of a delafossite-bearing sample from Sasca Montană
E7. táblázat. *A szászkabányai delafossittartalmú minta röntgen-pordiffrakciós adatai*